energies

MDPI

Article

A Preliminary Techno-Economic Comparison between DC Electrification and Trains with On-Board Energy Storage Systems

Regina Lamedica [1], Alessandro Ruvio [1,*], Manuel Tobia [1], Guido Guidi Buffarini [2] and Nicola Carones [2]

[1] Department of Astronautical, Electrical, and Energy Engineering, Sapienza University of Rome, 00185 Rome, Italy; regina.lamedica@uniroma1.it (R.L.); tobiamanuel@gmail.com (M.T.)

[2] Italferr S.p.A., 00155 Rome, Italy; g.guidibuffarini@italferr.it (G.G.B.); n.carones@italferr.it (N.C.)

* Correspondence: alessandro.ruvio@uniroma1.it

Received: 17 October 2020; Accepted: 15 December 2020; Published: 18 December 2020

Abstract: The paper presents a preliminary technical-economic comparison between a 3 kV DC railway and the use of trains with on-board storage systems. Numerical simulations have been carried out on a real railway line, which presents an electrified section at 3 kV DC and a non-electrified section, currently covered by diesel-powered trains. Different types of ESS have been analyzed, implementing the models in Matlab/Simulink environment. A preparatory economic investigation has been carried out.

Keywords: railway system; energy storage system (ESS); lithium batteries; supercapacitor; Simulink; sizing; catenary-free

1. Introduction

The International Energy Agency and the International Union of Railways have stated that the 23.1% of worldwide CO_2 emissions from fuel combustion are attributable to the transport sector (8258 million tons of CO_2). The breakdown of the emissions in this sector is attributable as follows: 73.2% to road transport, 10.4% to maritime transport, 10.5% to air transport and 3.6% to railways [1]. Regarding the European situation, the amount relating to the transport sector is around 30.4% (71.1% road transport, 13.9% maritime transport, 12.7% air transport and 1.5% railways). In the United States, the transport sector accounts for 34.4% of emissions from fuel combustion, in Japan for 20.6%, in Russia for 17.5%, in India 12.7% and in China for 9.6% [2,3]. According to the Statistical Compendium on Transport published annually by the Commission, net of emissions indirectly attributable to rail transport (which are accounted in electricity generation phase), therefore 44% of total emissions are attributable to road passenger transport, 28% for road freight, while air and maritime transport accounted for 13.0 and 13.4%, respectively. Overall, urban mobility would account for 25% of greenhouse gas emissions from transport, interurban for 54% and intercontinental for 22%) [1,4].

From the point of view of railway line electrification, Europe has 55% of the total length of the railway line electrified. Italy has 72% of electrified lines and 28% with diesel-powered trains [5].

E-mobility will be widespread thanks to the European Union funding programs and capital investments from the automotive industry. However, several technical, financial and social challenges need to be overcome. Although electric vehicles present higher purchase and infrastructure costs, they present lower operating costs than a conventional car [6–8]. Due to the limited autonomy and required charging times, battery electric vehicles are indicated for consumers with a limited daily range, but the technology, especially for storage systems, is constantly improving. In the long term, options like plug-in hybrid vehicles are expected to have a relatively big market share [9].

The worldwide diffusion of electric vehicles is still very limited. One of the main reasons of different trends in the sales of electric cars is the presence in some parts if the world of incentive mechanisms such as purchase incentives and free access to controlled priority circulation zones. Another relevant factor is the presence of proper charging infrastructures, which requires the companies involved to adapt their business models [10].

One of the main target areas of the climate goals is road freight transport, since about 25% of the CO_2 emissions from road transport in the European Union are produced by heavy-duty vehicles. Although shifting from road freight transport to electrified railways is a possible solution, several studies indicate that the potential for this is limited. New technologies such as electrified highways (eHighways) are proposed, in which an overhead line supply energy to trucks provided with an integrated pantograph. A two-pole catenary system has been developed, ensuring a stable current transmission at speeds up to 100 km/h [11]. This technology is already being used in several projects in countries such as Sweden and United States [12], and several such projects are in the planning phase.

The design of electrified mass transit systems for urban railway traffic, such as trams, trolleybuses and metros, requires taking into consideration several elements: safety, efficiency, cost and visual impact. Traditional electrified transit systems are based on electrical contact wires, such as active rails or catenary. Catenary-free systems have advantages of as low electromagnetic radiation and good visual design [13] In the absence of fixed traction systems, the rolling stock has on board the energy storage system (e.g., batteries, hydrogen, diesel, ultracapacitors, flywheels). Moreover, catenary-free systems are being consolidated in public transportation, especially to restrict the electrical infrastructure, for example in city historical centers, limiting the environmental impact and reducing costs of electrical installations for traction [14].

In the current state some form of on-board storage system is often used for heavy traction (passenger and freight trains), but generally only to recover braking energy and not to operate in catenary-free mode. Battery-powered locomotives were one of the first technologies to be adopted in the early 1900s but due to the limited storage capacity available at that time, it was decided to focus on electrified solutions. Use thus became limited to mining locomotives and shunting locomotives [15].

Nowadays several studies have focused on the possibility to design new trains to operate autonomously because of the advances in energy storage technologies [16]. Trains with on-board storage systems could be adopted for expansion of already electrified railways, point-to-point connections or commuter transport systems [17–19]. It will be important in the near future to considerate the need for prospective analysis of the marketing of rolling stock approved for bimodal operation (i.e., with and without contact lines supplying different voltages). The diffusion of a new system will strongly depend on the cost and the development of new rolling stock with on board storage technology for traction [20–22].

It is well known that for heavy traction, the electrified solution via catenary represents a consolidated and highly reliable approach that is economically sustainable for high traffic lines [23,24]. Moreover, considering the contribution of renewable sources it is possible to increase the energy savings from the primary network. For this reason, several studies and projects have been carried out highlighting the trend of replacing diesel locomotives with electric locomotives to cover long distances, powered by AC or DC electrification systems [25].

For solutions involving on-board energy storage systems (ESS), several technologies can be used, as shown in Figure 1. Since each one of them presents different characteristics, it is important to choose the most suitable technology for the particular case under study. Currently, there are different types of electrochemical accumulators. Lead-acid accumulators, widely used in the automotive sector, represent an economical and reliable solution. However, they have a very low specific energy. Those with nickel cadmium (Ni-Cd), initially used as substitutes for the aforementioned lead-acid accumulators, have been nowadays abandoned due to the toxicity of the cadmium present in them, and the focus has shifted to nickel-metal hydride accumulators (NiMH), which have the disadvantage of presenting memory effects. Finally, lithium batteries (Li-ion) are characterized by high energy and specific power.

Technologies such as flywheels offer a high specific power and a large number of charge and discharge cycles but they present low specific energy. The use of fuel cells in railway transport systems is currently in the early development state and they present many advantages such as zero emissions fuel and high specific energy [26]. Though fuel cell sources can be coupled with high-power density storage elements [27], the combination of Li-ion batteries with supercapacitors (SC) is currently found to be the most economical solution for ESS [26].

Supercapacitors, also known as ultracapacitors, are an innovative electrical EES that has considerably higher capacity values than those of ordinary capacitors and high specific power. The combination of Li-ion batteries and SC in a hybrid energy storage system (H-ESS) allows one to reduce battery stress and aging effects, depending on the charge and discharge cycles. The sizing of the ESS is strictly linked to the control strategy used for the management of energy resources and is limited by the maximum weight and volume allowed by the rolling stock [28,29].

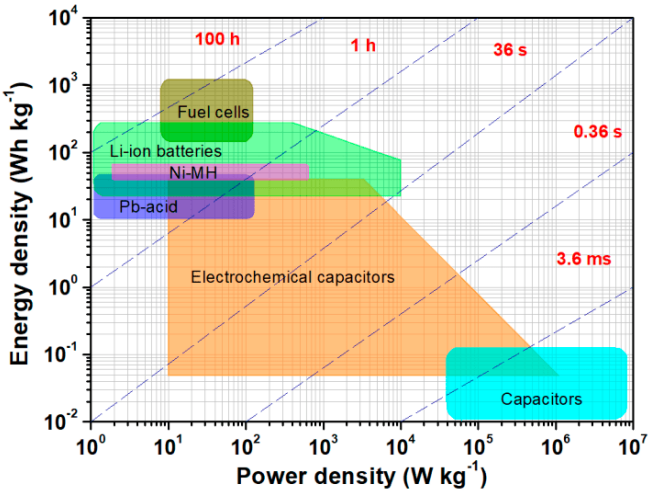

Figure 1. Ragone chart [30].

Several studies have been carried out on the applications of storage systems that use lithium-ion cells with high specific power (power-oriented) or high specific energy (energy-oriented). Usually, energy-oriented lithium-ion cells are accompanied by supercapacitors, which deliver the stored energy during power peaks in traction and absorb energy during regenerative braking [31,32]. It is possible to find different applications on electric vehicles [33,34], electric buses [35], small boats [36], water buses [37], and even machines for lifting and displacement of loads [38].

In [39], a battery pack of about 250 kWh and about 2 tons of mass is used on a freight train, in order to solve the problem of the absence of the catenary in the connections of the railway lines to the freight terminals and production plants, avoiding the use of diesel-powered vehicles. In [40], prototypes of battery packs of 200 kWh and about 2 tons are reported for a railway locomotive and of 500 kWh and 5 tons of mass for powering a mining truck. In [41], the authors present a battery pack of 2.22 MWh and 11 tons of mass to power a rolling stock with a total mass of 276 tons that must travel a route of 212 km.

Among the few solutions commercially available for trains equipped with energy storage systems there is a Spanish tramway in Seville, which uses a hybrid storage system consisting of supercapacitors and batteries [42]. In addition, the same train constructor has developed a battery-powered regional train, proposing it as a solution for non-electrified railway lines. The roof-mounted traction batteries provide the power and energy required to propel the train for distances up to 100 km [43,44]. It is important highlight that the adoption of storage system on board trams and trolleybuses is economically convenient for short route sections. There are already design solutions and rolling stock equipped with on-board storage systems available on market.

In addition to the technical and infrastructural characteristics of a given traction system, it is important to carry out a cost assessment, especially when comparing different achievable solutions. In the technical and scientific literature, several studies have been published using the annual cost of energy (ACOE) in order to evaluate the effectiveness in terms of costs of different types of energy resources [45]. In this study, the ACOE is also used to compare the different technical solutions proposed.

This paper presents the evaluation taken into consideration to perform a comparison between direct current electrification and the use of trains with on-board energy storage systems. Numerical simulations have been performed on a real railway line to carry out a preliminary techno-economic comparison showing the models and procedure used. The case study presents an electrified 3 kV DC section and a non-electrified section, currently being covered by diesel-powered trains. For the non-electrified section, the following scenarios have been analyzed: 3 kV DC electrification, since it is the feeding system currently used in the preceding section; high autonomy ESS and ESS with recharge station. For the ESS it has been considered the use of power-oriented Li-ion battery cells and, in the case of hybrid ESS, energy-oriented Li-ion battery cells accompanied by supercapacitors. For the sake of simplicity, only recharging the ESS has been considered, the possibility of swapping the ESS is outside the scope of this work, as it would have an impact on capital costs. It is highlighted that, in cost assessment is not taken into account the cost associated with the purchase of new trains. In this paper, it is assumed that the cost of the on board ESS is the difference cost between traditional electric trains and new trains equipped with on board ESS.

The paper is structured as follows: Section 2 describes the electric models of the vehicle, energy storage systems and DC feeder system, as well as the economic model. Section 3 presents the on-board ESS sizing procedure. Section 4 introduces the simulation software and procedures while Section 5 presents the case study and the numerical results of the simulations. Section 6 concludes the paper.

2. Modeling of the Railway System

The proposed model is obtained by using three different sub-models: the railway vehicle and its kinematics, the DC feeder system and the on-board ESS. An economic model is also introduced for calculating the annual energy cost of the proposed solutions.

2.1. Train

The longitudinal dynamic of vehicles is evaluated applying Newton's second law and kinematic equations:

$$\begin{cases} m\,\varepsilon\frac{dv}{dt} = F(t) - R_{BASE}(v) - R_{TRACK}(x) \\ x = x_0 + v_0\,t + \frac{1}{2}\frac{dv}{dt}\,t^2 \\ v = \frac{dx}{dt} \end{cases} \quad (1)$$

where m is the mass of the vehicle, ε is a correction factor taking into account the rotating mass, v and x are the train speed and position respectively, F is the traction (if positive) or braking (if negative) force. $R_{BASE}(v)$ is the basic resistance including roll resistance and air resistance, and $R_{TRACK}(x)$ is the line resistance caused by track slopes and curves, described by:

$$R_{BASE}(v) = \alpha_1 + \alpha_2|v| + \alpha_3 v^2 \quad (2)$$

$$R_{TRACK}(x) = mg\,sin(\gamma(x)) + mg\frac{a}{r(x) - b} \quad (3)$$

where α_1, α_2 and α_3 are the coefficients of the Davis formula, related to the train and track characteristics, and they can be estimated by empirical measures; g is the gravitational acceleration and $\gamma(x)$ is the slope grade. The second term of R_{TRACK} is the curve resistance given by empirical formulas, as the Von Röckl's formula, where $r(x)$ is the curvature radius, and a, b are coefficients which depend on the track gauge; in this paper it is considered a = 0.65 m and b = 55 m [46].

From a given a speed cycle, it is possible to calculate the value of the force (F_{MECH}) on the wheels required to overcome the vehicle inertia, slopes and curves, aerodynamic friction and rolling friction. Going upstream the vehicle components and their related efficiencies, the power requested to the contact wire P_{TRAIN} is calculated as follows:

$$P_{TRAIN} = \begin{cases} \frac{F_{MECH}\, v}{\eta_t} + P_{AUX}, & F_{MECH} \geq 0 \\ (F_{MECH}\, v)\, \eta_t + P_{AUX}, & F_{MECH} < 0 \end{cases} \quad (4)$$

where P_{AUX} is the power absorbed by board auxiliary services (lighting, cooling or heating), m is the total mass of the train (including the passengers), v is the vehicle speed and η_t the total efficiency of the locomotive, which takes into account the efficiency of the gear box, the electric motor and the inverter. To bring into account that the voltage along the track is not constant, the railway vehicle is modeled as an ideal current source I_{TRAIN}, whose is calculated as the ratio between vehicle power and line voltage V_{LINE}:

$$I_{TRAIN} = \frac{P_{TRAIN}}{V_{LINE}} \quad (5)$$

2.2. DC Feeder System

Conventional substations are represented by ideal DC voltage sources, series resistance and series diode if the substations are not reversible [28]. The contact wire is modelled as a set of electric resistances that change their value according to the vehicle position. If $x(t)$ is the train position at the time t, the value of the resistance upstream R_a and downstream R_b to the vehicle towards a generic node of the railway feeding system (conventional substation or another train) are calculated by:

$$\begin{cases} R_a(t) = \rho \cdot x(t) \\ R_b(t) = \rho \cdot [d - x(t)] \end{cases} \quad (6)$$

where R_a and R_b are expressed in [Ω], ρ [Ω/km] represents the resistive coefficient, d [km] is the distance between the two nodes (upstream and downstream the train). In order to improve the train electric model, describing the receptivity of the network under regenerative braking conditions, a small capacitance is connected in parallel to current source that represents the vehicle [46]. In Figure 2 it is shown the electric model of the overall railway system, one side supplied contact line.

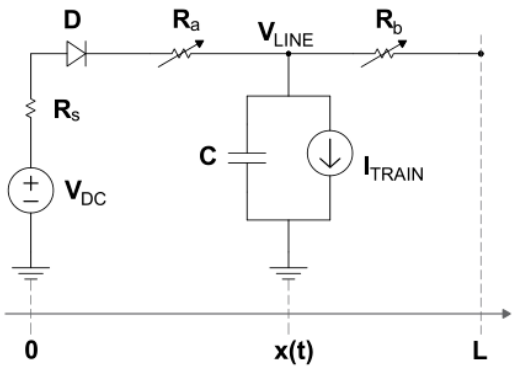

Figure 2. Electric model of the one side DC supplied contact line.

2.3. On-Board ESS

The electric model of the ESS is reported in Figure 3, it includes the battery and supercapacitor pack, the DC/DC converter and the power flow controller. The on-board ESS is modelled as a pair of ideal current sources describing the battery-based and the SC-based energy storage system, respectively.

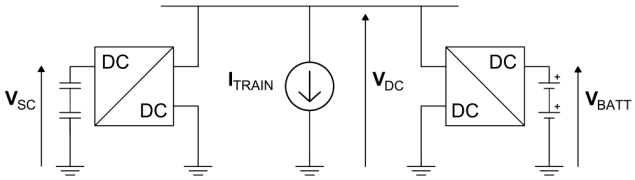

Figure 3. On-board Hybrid ESS electric model.

Figure 4a presents the equivalent circuit of the battery pack, which consists of an ideal voltage source that represents the open circuit voltage (OCV), which depends on battery state of charge (SOC); the series resistor R_{INT} represents the internal resistance, whereas r_d and C_d are the RC parallel circuit describing the charge transfer and double layer capacity, respectively. The set of equations that describes the electric model of the battery pack is reported in Equations (7) to (10): the first equation represents Kirchhoff's voltage law, the second one is the n-polynomial relationship between OCV and SOC. The third equation models the SOC update law according to the required current from the battery pack and the last one is the differential equation describing the RC parallel circuit [29].

$$V_{BATT}(t) = OCV(t) - R_{INT}I_{BATT}(t) - u_d(t) \tag{7}$$

$$OCV(\mathrm{SOC}) = \beta_n \mathrm{SOC}^n + \beta_{n-1}\mathrm{SOC}^{n-1} + \beta_0 \tag{8}$$

$$\mathrm{SOC}(t) = \mathrm{SOC}(t=0) - \frac{1}{3600 \cdot C_{AH}} \int_0^t I_{BATT}(\tau)d\tau \tag{9}$$

$$u_d(t) + r_d C_d \frac{du_d(t)}{dt} = r_d I_{BATT}(t) \tag{10}$$

where $u_d(t)$ is the r_dC_d parallel circuit voltage, $\beta_0 \ldots \beta_n$ are the interpolation coefficients and C_{AH} [Ah] is the battery pack capacity. The electrical model of the SC pack, shown in Figure 4b, consists of the capacitor C, modelling SC's capacity; an equivalent series resistance R_S that describes the power loss during the charging and discharging operations; the self-charge resistance R_L models the losses due to the leakage current, which is usually neglected [28,47]:

$$V_{SC}(t) = V_C(t) - R_s I_{SC}(t) \tag{11}$$

$$V_C(t) = V_{SC}(t=0) - \frac{1}{C}\int_0^t I_{SC}(\tau)d\tau \tag{12}$$

$$\mathrm{SOC}_{SC}(t) = \frac{1}{3}\left[4 \cdot \left(\frac{V_C(t)}{V_{nom}}\right)^2 - 1\right] \tag{13}$$

(**a**) (**b**)

Figure 4. Equivalent circuit of the battery pack (**a**) and SC pack (**b**).

It is highlighted that, in order to represent the equivalent circuit of a battery or supercapacitor pack, starting from the characteristics associated with the individual cells or modules, it is used an equivalent circuit: n RC blocks in series and m in parallel [48]. The DC/DC converters are modeled by its average efficiency η describing power losses. It operates as step-up or step-down converter according to the control characteristic. Given the power reference value P_{ref} provided by the power flow control characteristic, the ESS current value to be delivered during the traction phase is computed by using the following equation:

$$I_{ref} = \frac{1}{\eta}\frac{P_{ref}}{V_t} \tag{14}$$

where V_t is the battery pack or supercapacitor pack voltage.

2.4. Economic Model

The annual cost of energy is used to compare the different technical solutions proposed. Therefore, it is necessary to estimate the present value of the total cost, which includes: the cost of capital, the present value of the operating costs and the present value of the replacement cost of the energy storage system [45]. The ACOE is mathematically expressed as:

$$ACOE = CRF \cdot C_{TOT} \tag{15}$$

where CRF is the capital recovery factor converting a present value into a stream of equal annual payments over a specified lifetime N, at a specified interest rate r, and C_{TOT} is the present value of the total cost. The capital recovery factor is computed by using the following equation:

$$CRF = \frac{r(1+r)^N}{(1+r)^N - 1} \tag{16}$$

2.4.1. Costs of an Electrified Railway Line

Measuring the performance of an electrified railway is particularly complex as it involves a service that requires rolling stock, tracks, safety and signaling systems, stops or stations, and a variety of personnel types. Another factor that affects transport, if it is public, is government intervention to subsidize costs [49]. In the present study, the cost of capital associated with fixed electrical systems has been estimated based on the main components that characterize this scenario:

$$C_I^{ELE} = C_{TPS} + C_{CAT} + C_{MSC} \tag{17}$$

where C_I^{ELE} is the capital cost of the electrification of the railway line, C_{TPS} is the cost associated with the traction power substation, C_{CAT} is the cost associated with the installation of the catenary and C_{MSC} represents other costs related to the electrification intervention such as track lowering in correspondence of tunnels already present in the route and raising of the overpasses. The present value of operation and maintenance (O&M) costs associated with the electrified railway line is calculated as follows:

$$C_{O\&M}^{ELE} = \sum_{n=1}^{N} \frac{C_n^{ELE}}{(1+r)^n} \tag{18}$$

where C_n^{ELE} is the annual operations cost of year n including both fixed and variable costs:

$$C_n^{ELE} = C_e N_d E_d^{TPS} + C_n^{TPS} + C_n^{CAT} \tag{19}$$

where E_d^{TPS} is the energy supplied by the traction power substation in a day, during N_d days within a year, C_e the average cost of electricity, C_n^{TPS} and C_n^{CAT} represent the average of the annual costs associated with the maintenance of the traction power substation and the catenary, respectively,

estimated from 1% to 3% per year of the investment cost, referring to the date of commissioning of the equipment [50]. Finally, the annual cost of energy is calculated by using the following equation:

$$ACOE_{ELE} = CRF \cdot \left(C_I^{ELE} + C_{O\&M}^{ELE} \right) \tag{20}$$

2.4.2. Costs of Associated with the Use of Trains Equipped with On-Board ESS

The costs taken into account are the capital cost of the on-board ESS, the annual operation costs of the on-board ESS, operation and maintenance (O&M) costs of the on-board ESS and the replacement cost of the on board ESS.

The use of trains equipped with ESS might reduce capital costs as there is no catenary, but the construction of new specialized trains could significantly increase the total costs of realization. Moreover, depending on how the sizing of the energy storage system is carried out, it may be necessary to install a charging system with an installed power comparable to that of a traction power substation, thus affecting capital costs. Furthermore, it is necessary to respect the limits of the state of charge within which the ESS must deliver and absorb energy, even with high discharge current peaks provided they occur for short periods of time, resulting in a useful life of 10÷15 years [51]. However, is needed an expertise in train operation and real work cycle of storage system to know if this useful life is respected.

Consequently, the cost assessment must include the future replacement of the energy storage system following life expectancy and battery life reported in data sheet (not considering battery disposal).

In cost assessment is not taken into account the cost due to the buy of new trains, but is assumed that the cost of the on board ESS is the difference cost between traditional electric trains and new trains equipped with on board ESS. So, the following analysis is relevant on the hypothesis of complete renewal of the rolling stock, as diesel trains.

The cost of capital of the equipment of the storage systems C_I^{ESS}, has been estimated as follows:

$$C_I^{\text{ESS}} = C_P P_{\text{ESS}} + C_E E_{\text{ESS}} + C_{FC} \tag{21}$$

where C_P [€/kW] and C_E [€/kWh] are the ESS specific costs, P_{ESS} and E_{ESS} are the power and energy capacities and C_{FC} are the ESS fixed costs associated, for example, with the installation of a recharging system. The present value of operation and maintenance costs associated with the use of trains equipped with on-board ESS $C_{O\&M}^{\text{ESS}}$, is calculated by:

$$C_{O\&M}^{\text{ESS}} = \sum_{n=1}^{N} \frac{C_n^{\text{ESS}}}{(1+r)^n} \tag{22}$$

where C_n^{ESS} is the annual operations cost of year n including both fixed and variable costs, and is computed by using the following equation:

$$C_n^{\text{ESS}} = C_f P_{\text{ESS}} + C_v N_d \, E_d^{\text{ESS}} + N_d \, \frac{E_d^{\text{ESS}}}{\eta_{ch}} C_{ch} \tag{23}$$

where C_f [€/kW-yr] represents the specific operating costs, C_v [€/kWh] the variable operating costs, C_{ch} [€/kWh] the cost of recharging ESS, N_d the number of days the ESS is active within one year, P_{ESS} [kW] and E_d^{ESS} [kWh] the nominal power and energy supplied by the ESS, and finally η_{ch} is the charge efficiency. The replacement cost of the ESS is expressed in the following equation:

$$C_R^{\text{ESS}} = C_{FR} \left[(1+r)^{-L_R} + (1+r)^{-2L_R} + \ldots \right] \tag{24}$$

where C_{FR} represents the future value of replacement cost and L_R is the ESS lifetime. Finally, the annual cost of energy is calculated by using the following equation:

$$ACOE_{\mathrm{ESS}} = CRF \cdot \left(C_I^{\mathrm{ESS}} + C_{O\&M}^{\mathrm{ESS}} + C_R^{\mathrm{ESS}}\right) \tag{25}$$

3. On-Board ESS Design

In the railway sector, the applications of electrical energy storage systems are usually characterized by the power and energy they must provide. A good sizing of the ESS must allow compliance with the required energy and power constraints, without too many margins.

3.1. ESS Specification

The sizing is performed considering a nominal voltage for the battery pack and for the supercapacitor pack, and a power profile assigned for each [28,32]. The subdivision of the original power profile is achieved through a low pass filter and an amplitude limiter [47,52,53]. Several optimization studies have been carried out on this topic [32,35,54]. In this paper, it is considered that the ESS may be composed of high-power lithium-ion cells or high-energy lithium-ion cells and supercapacitors (H-ESS). Shape and weight of the energy storage system are binding constraints since they limit the energy that can be stored on-board. Therefore, the sizing depends on several factors: autonomy and maximum power required; where the charging is performed; the type of storage system.

3.2. ESS Sizing

Given a commercial battery cell characterized by a nominal cell voltage U_{CELL_B} the number of cells to be connected in the series N_{SE_B} to obtain a given rated voltage of the battery pack, U_B is obtained by:

$$N_{SE_B} = \frac{U_B}{U_{CELL_B}} \tag{26}$$

It is highlighted that it represents a simplified model for the preliminary study developed in this paper, but in the case of a cell pack, balancing and operating safety should be added. The number of branches to be connected in parallel N_{PAR_B} is determined as the maximum number between $N_{PAR_B}^P$, which represents the number of branches in parallel to satisfy the power requirement to be delivered in traction P_B^{max}, and $N_{PAR_B}^E$ which is the one necessary to satisfy the energy required by the battery, E_B. In order to increase battery lifetime, the variations in the state of charge are limited between a SOC_{min} of 0.2 ÷ 0.3 and a SOC_{max} of 0.8 ÷ 0.95. This involves an oversizing with respect to the energy required by the reference cycle but allows to exploit the supply or absorption of high currents for short intervals of time, provided that the fluctuations in the SOC are less than 5% (micro-cycles). An energy storage system of this type, subject to this type of stress, has an expected useful life of 10 ÷ 15 years [51,52,55]. Moreover, several studies have been carried out evaluating the use of degraded batteries, since they still have remaining capacity for grid support applications or emergency power supply [56–58]:

$$N_{PAR_B} = \max(N_{PAR_B}^P;\ N_{PAR_B}^E) \tag{27}$$

$$N_{PAR_B}^E = \frac{E_B}{N_{SE_B} \cdot U_{CELL_B} \cdot C_{AH_{CELL_B}} \cdot (\mathrm{SOC}_{max} - \mathrm{SOC}_{min})} \tag{28}$$

$$E_B = \int_{t_0}^{t_0+T} P_B(t)dt \tag{29}$$

$$N_{PAR_B}^P = \frac{P_B^{max}}{N_{SE_B} \cdot P_{CELL_B}^{max}} \tag{30}$$

where $P_{CELL_B}^{max}$ is the maximum power that the single electrochemical cell can deliver, determined in the discharge phase by using Equation (31), where R_{DIS} [h^{-1}] is the discharge C-rate, which is a measure of the rate at which the cell is discharged relative to its nominal capacity $C_{AH_{CELL_B}}$ [Ah]. The maximum power that the single cell can absorb in the charging phase is computed as a function of the charge C-rate R_{CH} [h^{-1}] [31]:

$$P_{CELL_{B_{DIS}}} = R_{DIS} \cdot C_{AH_{CELL_B}} \cdot U_{CELL_B} \quad (31)$$

$$P_{CELL_{B_{CH}}} = R_{CH} \cdot C_{AH_{CELL_B}} \cdot U_{CELL_B} \quad (32)$$

Given a commercial supercapacitor of rated voltage $U_{CELL_{SC}}$, the number of cells to be connected in series $N_{SE_{SC}}$ to obtain a given rated voltage of the supercapacitor pack U_{SC} is determined by:

$$N_{SE_{SC}} = \frac{U_{SC}}{U_{CELL_{SC}}} \quad (33)$$

The number of supercapacitor branches to be connected in parallel, $N_{PAR_{SC}}$, is determined through Equation (34), where E_{SC_max} is the maximum energy that the supercapacitor pack must deliver. It is highlighted that the voltage range is limited between $V_{NOM}/2$ (SOC_{SC} = 0) and V_{NOM} (SOC_{SC} = 1), delivering 75% of the stored energy:

$$N_{PAR_{SC}} = \frac{8}{3} \frac{E_{SC\_max}}{(N_{SE_{SC}} \cdot U_{CELL_{SC}})^2} \cdot \frac{N_{SE_{SC}}}{C_{CELL}} \quad (34)$$

$$E_{SC}(t_p) = \int_{t_0}^{t_0+t_p} [P_{SC}(t) - P_{SC}(t_0)] dt \quad (35)$$

Finally, the total mass W_{TOT} and volume V_{TOT} linked to each energy storage system can be computed as follows:

$$W_{TOT} = (1+\gamma) \cdot N_{SE} \cdot N_{PAR} \cdot W_{CELL} \quad (36)$$

$$V_{TOT} = (1+\delta) \cdot N_{SE} \cdot N_{PAR} \cdot V_{CELL} \quad (37)$$

where the coefficients γ and δ represent mass and volume rations of DC/DC converters and all the other additional elements necessary for the assembly and use of the energy storage system.

4. Simulation Procedures

The railway system model was implemented in a rail simulator based on the 'quasi static' backwards looking method, due to its short simulation times for estimating energy consumption of vehicles following an imposed speed cycle [46]. The rail simulator is a multi-stage program, implemented in Visual Basic and Fortran language and operating in MS-DOS and the Microsoft Excel workspace [59–61], including:

- an electro-mechanical simulator for the evaluation of the rolling stock power consumption for defined traffic scenarios;
- an electrical and thermal simulator to evaluate the energy state of the traction system.

The software allows one to perform high-quality studies from an energy point of view, with a high degree of flexibility in the simulation by means of a graphical interface where it is possible to set many parameters such as trains' departure times, specific train sequences and trains' stop time period in each station.

For the sizing and verification of the energy storage systems, models have been implemented in the Matlab/Simulink environment. Given the parameters of the electrochemical cells and supercapacitors, and given the power profile to be supplied, it is possible to evaluate electrical variables such as voltage, current, state of charge, power and energy supplied and absorbed.

The numerical simulations have been divided into three parts. The first part is related to the train performance simulations, to determine the power profile required by the rolling stock. The second part is related to the traction system simulations, in which the system is studied from an energy point of view, inserting traffic data and imposing simulation constraints. The last part is related to the on-board energy storage systems, which presents the ESS performance given a power profile reference.

4.1. Train Performance Simulation

The train performance, computed in the Microsoft Excel environment, requires the main characteristics of the route as input data, namely the plano-altimetric characteristics of the line (slopes), the curvature radius of the curves, speed limits and tunnels. Moreover, it requires electromechanical information of the rolling stock such as: weight, aerodynamic resistance, traction and braking force [46,59]. Given these inputs, and with a calculation step in meters, it is possible to obtain several outputs such as:

- kinematic parameters: travel and braking times, speed and acceleration profiles in time and space;
- dynamic parameters: aerodynamic resistance, resistance associated with curves, slopes and inertia, traction effort at the wheels and power required at the pantograph.

4.2. Electrical Model of the Traction System

The electrical computation software, implemented in Fortran language, allows to solve load flows calculation for a direct current electrified system [46,60,61]. For each simulation step, the software creates an equivalent electric network in which the nodes represent the traction power substation, vehicles present on the route and parallel points, as shown in Figure 5. In this model, V_{TPS} and R_{TPS} represent the substation DC voltage and internal resistance; R_{BIN} is the rail electric resistance and P^{BIN} is the electric power required by each train.

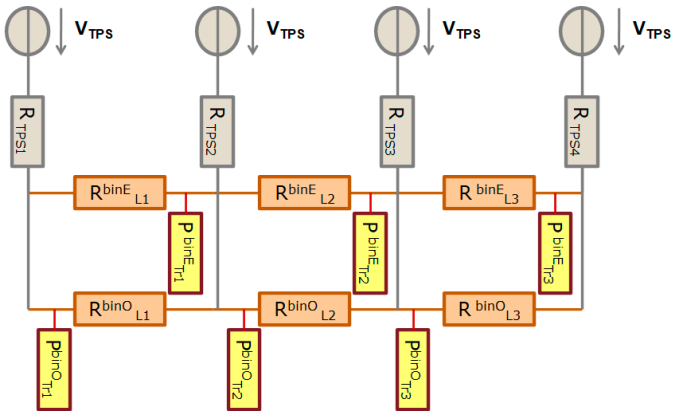

Figure 5. Electric software circuit model.

The software requires as input the data related to the power profiles of trains, the electrical substation features and the resistance of contact line equivalent section and rails. As output, the software provides the line voltage profile and currents flowing in the substation feeders, as well as the power provided by each electrical substation [61,62].

4.3. Electrical Model of the On-Board Energy Storage System

Simulink/Matlab models have been developed for the battery pack and supercapacitor pack, starting respectively from the characteristics of the electrochemical and supercapacitor cells. The models have been implemented as dynamic continuous-time systems, thus using mainly integrator, sum and gain blocks. In the case of electrochemical cells, a lookup table dynamic block is used to represent the

open circuit voltage as a function of the state of charge (OCV-SOC curves). Figure 6 shows the battery based ESS Simulink model.

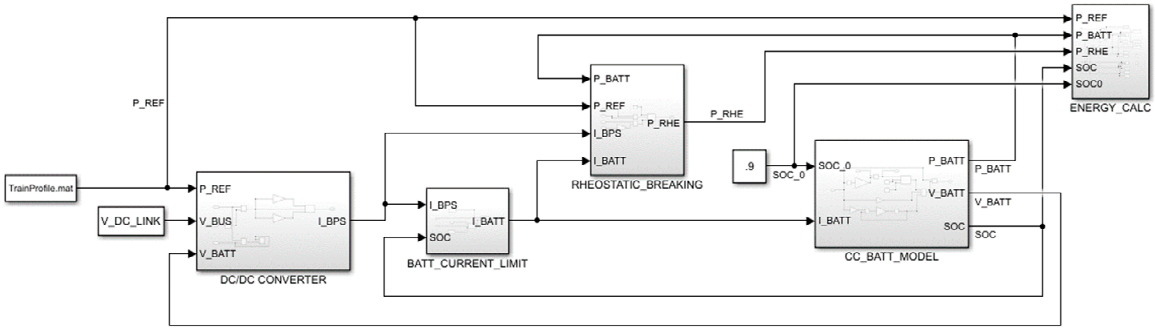

Figure 6. Battery based ESS Simulink model.

In addition to the parameters related to the energy storage system, the software requires as input data the reference power profile required, which is obtained directly from the evaluation of the train performance in the case of high-power lithium cells. In the case of H-ESS, the reference power profiles for the high-energy lithium cells and supercapacitors are obtained from a Simulink model that applies a low pass filter and an amplitude limiter to the original power profile.

5. Numerical Simulations

5.1. Case Study

A real single-track railway line has been chosen as case study. It presents an electrified section at 3 kV DC and a non-electrified section, currently covered by diesel-powered trains. Therefore, passengers are obliged to transfer to a diesel-powered train at the end of the electrified section, in order to reach one of the following stops or stations. The attention is focused to the non-electrified section in order to determine the technical-economic convenience of electrification at 3 kV DC or the use of trains equipped with on-board energy storage systems. Figure 7 reports an overview of the case study.

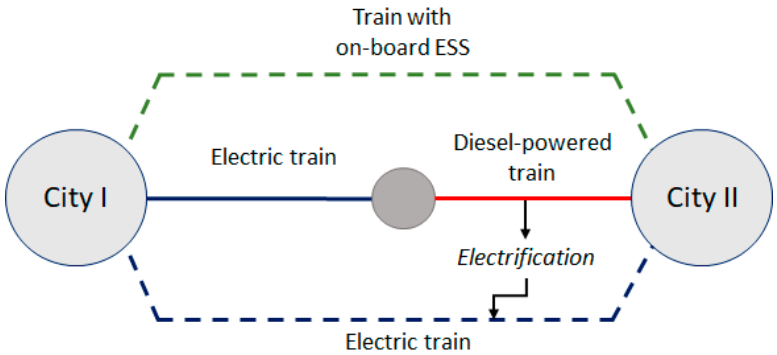

Figure 7. Railway connection between City I and City II and possible scenarios.

The non-electrified section is about 16.5 km long and links Station A, at the end of the electrified section with Station B, at the end of the non-electrified section (City II), in about 30 min for each direction. Between Station A and B there are 5 stops, as shown in Figure 8.

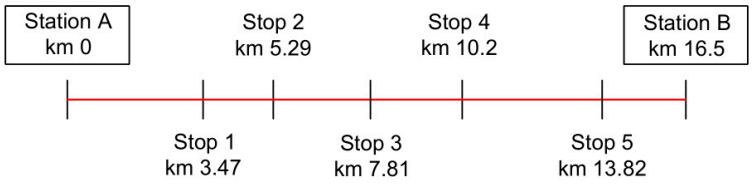

Figure 8. Stops between Station A and Station B.

Figure 9 shows the plano-altimetric profile of the railway line. It is characterized by an average slope of 9‰, with a maximum slope of 24‰. There are 22 curves with a minimum bending radius of 200 m.

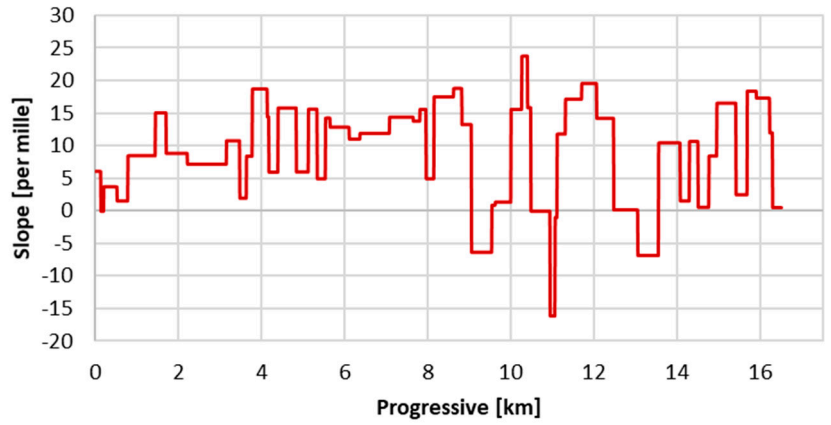

(**a**)

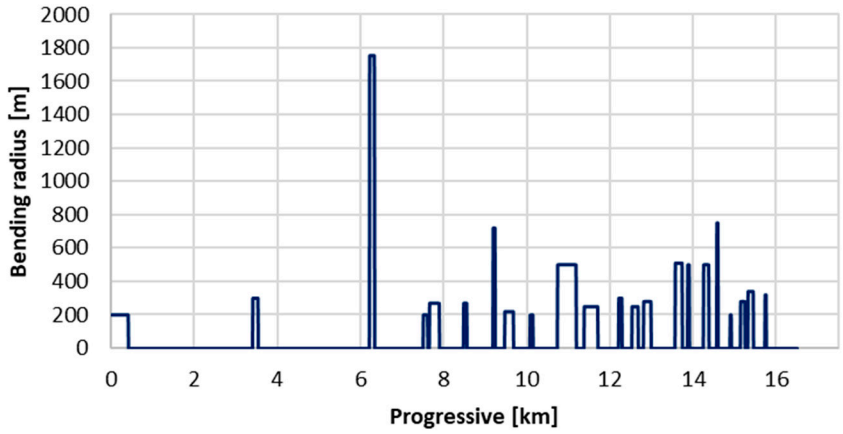

(**b**)

Figure 9. Track features: slopes (**a**) and curves (**b**).

For the non-electrified section, the following scenarios have been analyzed: 3 kV DC electrification, since it is the feeding system currently used in the preceding section; high autonomy ESS and ESS with recharge station. For the ESS it has been considered the use of power-oriented Li-ion battery cells (lithium iron phosphate, LFP) and, in the case of hybrid ESS, energy-oriented Li-ion battery cells (lithium nickel manganese cobalt oxide, NMC - lithium nickel cobalt aluminium oxide, NCA) accompanied by supercapacitors.

The electrification at 3 kV DC involves the installation of a catenary and traction power substation, to be located at Stop 2 (progressive km 5.29). Contrariwise, the use of trains equipped with high autonomy on-board ESS allows to minimize the capital costs since it involves the recharge of the battery and supercapacitor pack in the electrified section of the line. However, in this case the ESS weight is high. The installation of a charging infrastructure at Station B (progressive km 16.5), allows reducing the on-board ESS rated capacity and therefore, the total weight of the system. In this paper, it is considered for all the scenarios, the use of the same electric train, whose traction curve is presented in Figure 10.

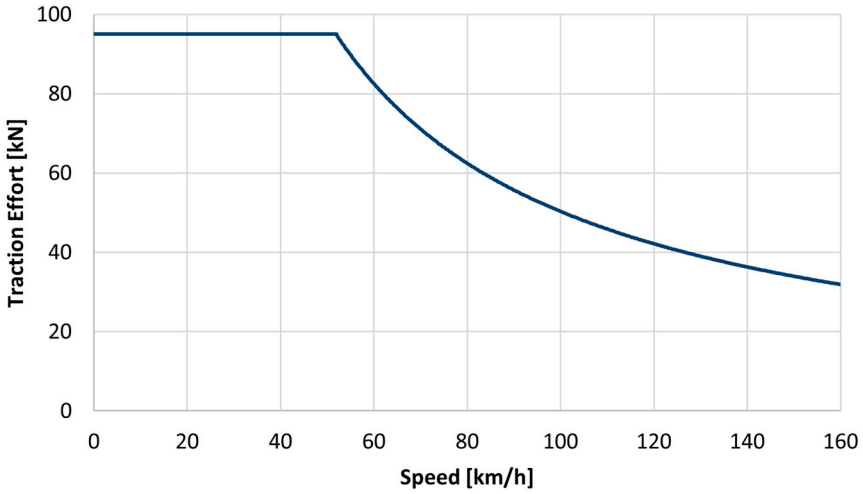

Figure 10. Rolling stock traction curve.

The main characteristics of the lithium-ion and supercapacitor cells are illustrated in Tables 1 and 2, respectively. This data is used to size the ESS as reported in the Section 3 of this paper. Table 3 shows the main characteristics of the different components of the traction system: rolling stock, track, DC feeder system and on-board ESS.

Table 1. Li-ion cell features.

Parameter	LithiumWerks ANR26650M1B	Saft MP 176,065 xlr
Mass [g]	76	150
Rated capacity [Ah]	2.5	6.8
Nominal voltage [V]	3.3	3.65
Specific energy [Wh/kg]	109	165
Max. discharge current [A]	50 (20C)	14 (2C)
Max. charge current [A]	10 (4C)	6.8 (1C)
Technology	Power-oriented	Energy-oriented

Table 2. Ultracapacitor cell features.

Parameter	Maxwell K2 UC–2.85V/3400F
Mass [g]	520
Rated capacity [F]	3400
Nominal voltage [V]	2.85
Max. voltage [V]	3
Specific energy [Wh/kg]	7.6
Specific power [W/kg]	8500

Table 3. Railway System Parameters.

Parameter	Value
Rolling Stock	
Net weight	184 t
Loaded weight	256 t
Rotating mass coefficient	1.05-
Max. train speed	160 km/h
Nominal deceleration	0.8 m/s^2
Accessories power	200 kW
Power train overall efficiency	0.8-
Track	
Track's length	16.5 km
Von Röckl formula coef. A	0.65 m
Von Röckl formula coef. B	55 m
DC Feeder System	
Catenary section	320 mm^2
Rail electric resistance	0.083 Ω/km
Substation location	5.29 km
Substation nominal power	3.6 MVA
AC/DC conversion units	2-
Substation DC voltage	3000 V
Substation internal resistance	0.2 Ω
Maximum line voltage (+20%-CEI EN 50163)	3600 V
Minimum line voltage (−33%-CEI EN 50163)	2000 V
On-board ESS	
DC link nominal voltage	3000 V
Max. (Min.) battery SOC value	90 (30)%
Battery pack nominal voltage	1500 V
Supercapacitor pack nominal voltage	1000 V
DC/DC efficiency	95%

5.2. Results and Discussion

Several simulations are carried out in order to determine the technical and economic convenience of the proposed scenarios, using the procedures reported on Section 4.

5.2.1. Train Performance

The train performance has been performed for each direction of travel: from Station A to Station B and vice versa. Figure 11 shows the speed profile from Station A to Station B, highlighting that the train that travels the line from one stop to another, accelerating until the speed limit is reached and decelerating accordingly of stops.

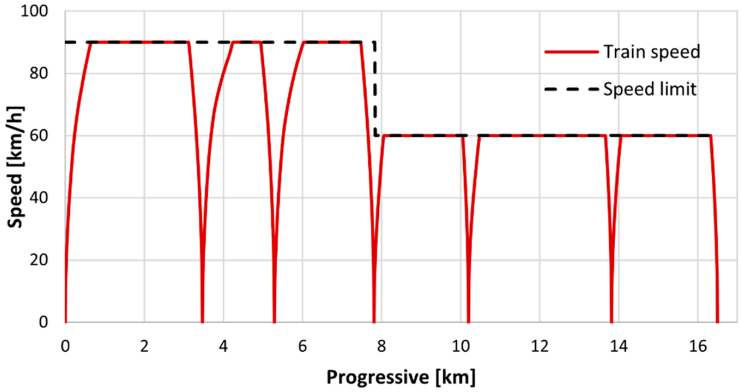

Figure 11. Speed profile from Station A to Station B.

Starting from the speed profile, it is possible to obtain the power profile of each direction of travel, as shown in Figures 12 and 13. For each single section present between one stop and another, the train uses all the effort theoretically available only in the acceleration phases until the limit speed of the track is reached. Subsequently, in the steady state phase, the tractive effort applied at the wheels follows the trend of the resistance offered by the various accidentalities present in the track, influencing the power requested by the train. It is also noted that the maximum power at the pantograph in the traction phase is 3.7 MW and the maximum power in the regenerative braking phase is 2 MW. During stops, the only power consumed by the train is related to auxiliary services.

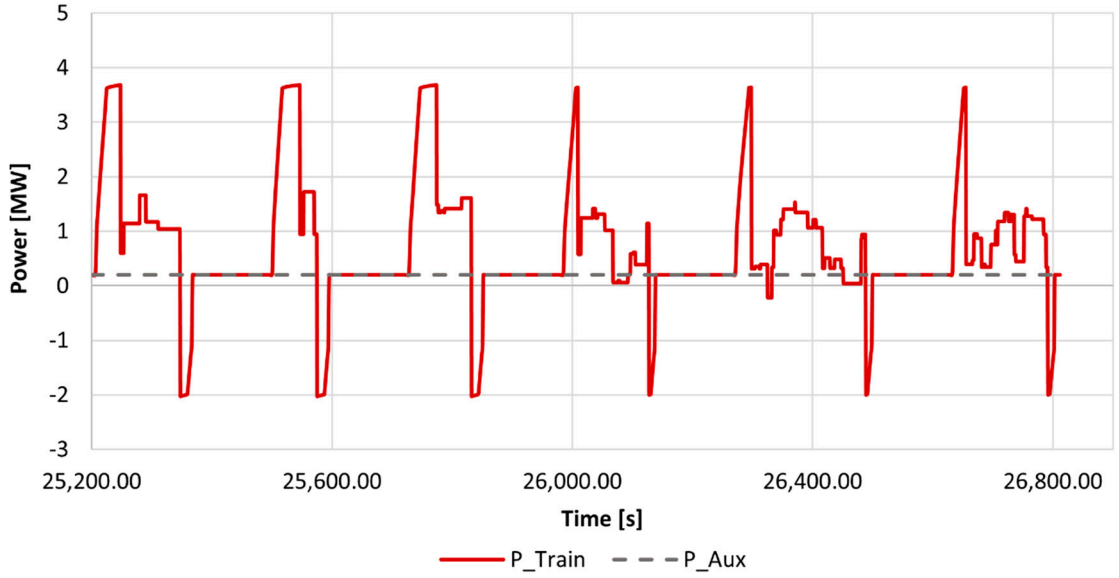

Figure 12. Power profile from Station A to Station B.

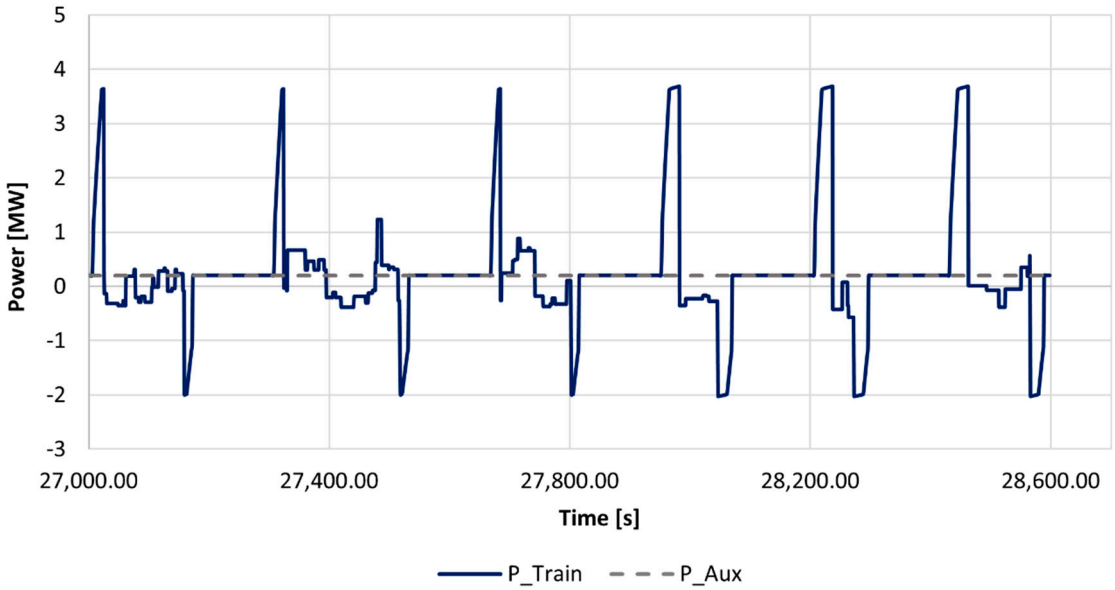

Figure 13. Power profile from Station B to Station A.

From Station A to Station B, the energy consumption is about double respect of the opposite direction, where the regenerative braking energy is high as the rolling stock must brake to contain its speed. It is due to the negative sign of the track resistance since the train goes downhill.

Figure 14a shows the energy consumption of the train and the regenerative braking energy, for each direction of travel. Figure 14b reports the timetable of the railway line under study (26 min and 51 s from Station A to Station B and 26 min, and 38 s in the opposite direction).

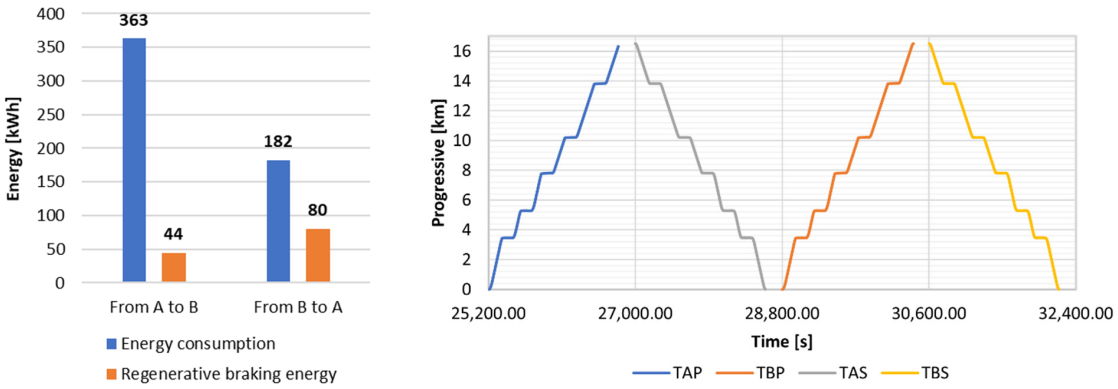

Figure 14. Energy required by trains: (**a**) Energy data; (**b**) Traffic conditions of the railway line.

5.2.2. Electrification at 3 kV DC

The electrification of the section under study include the installation of a traction power substation and the contact line. Therefore, it is necessary to determine the nominal power of the transformer groups present in the substation and the catenary to be used, considering the limits allowed by the CEI EN 50163 standards. For the TPS, located at Stop 2, it has been analyzed the use of two different types of substations: 2 AC/DC conversion units with a nominal power of 3.6 MVA or 5.4 MVA each. For the catenary, it has been considered the use of an equivalent section of 320 mm^2 or 440 mm^2. For simplicity purposes, only the numerical results related to the 2 × 3.6 MVA TPS with a 320 mm^2 are here reported.

Figure 15 reports the minimum line voltage, highlighting that the voltage drop along the line is critical only at 7:30 and 8:30, at the departure of the train from Station B, towards Station A. In this case, the TPS must feed the train that is more than 11 km away. In fact, it is necessary to limit the power to the pantograph to 3 MW in order to contain the voltage drop on the line, obtaining a voltage at the pantograph is 2.19 kV. However, this minimum voltage is present only for a single sample of the simulation (10 s).

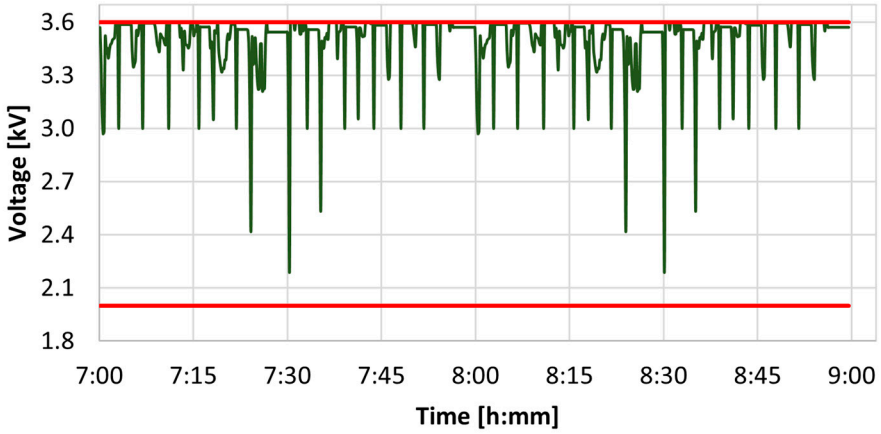

Figure 15. Minimum line voltage.

Figure 16 shows the TPS power absorption and given that the power required to the primary network does not exceed 10 MVA, it is possible to provide for the medium voltage connection to the primary network.

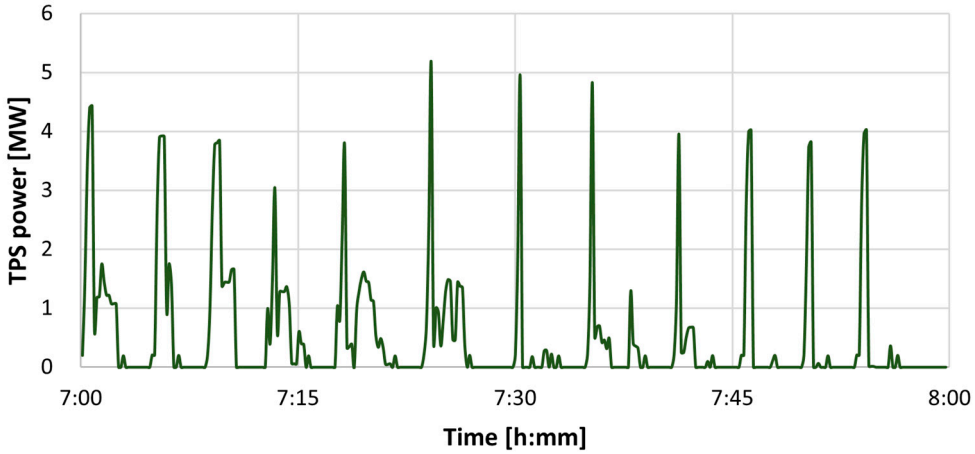

Figure 16. Power absorbed by the traction power substation between 7 a.m. and 8 a.m.

5.2.3. On-Board ESS

The main constraints of the on-board ESS sizing are the energy required by the cycle and the maximum power to be delivered. In the case of an electrochemical storage system, this must provide both the energy required by the cycle and the power during peaks related to accelerations. Instead, in the case of a H-ESS consisting of batteries and supercapacitors, the power profile required by the train is divided into two parts, obtaining a reference profile for the battery pack and another for the supercapacitor pack.

The high autonomy ESS implies an autonomy to go from Station A to Station B and recharge the storage system at Station A. According to this cycle, the energy to be supplied to the rolling stock is equal to 585 kWh. First, the use of high-power lithium-ion cells has been analyzed, whose characteristics are shown in Table 1. In this case, the sizing results in a 980 kWh (650 Ah) battery pack, of which only 586 kWh can be used, due to SOC limits. In Figure 17, P_{BATT} represents the power associated with the battery pack, positive in the traction phase, and negative in the braking phase. The voltage of the battery pack is identified as V_{BATT} and presents variations that re less than ±5%. The supplied current is identified as I_{BATT} and is positive in the discharge phase (traction) and negative in the charging phase (regenerative braking). Since the capacity of the battery pack (C) is equal to 650 Ah, it is observed that both the maximum discharge and charge current are much lower than the maximum allowed by the battery pack (20C and 4C respectively, in the discharge phase and charge). Moreover, it is observed that the sizing is appropriate because the SOC does not drop too low, and over time (despite greater discharges), the SOC will not drop below a certain minimum (30%).

Afterwards, a high autonomy H-ESS has been analyzed. It is composed of the high-energy lithium-ion and supercapacitor cells, whose characteristics are shown in Tables 1 and 2. The subdivision of the original power profile is achieved through a low pass filter with a cut-off frequency of 1 Hz and an amplitude limiter which limits the maximum power supplied by the batteries to reference value equal to 2 MW, in order to reduce the maximum power peak that they must supply to about 50% of the original one. Instead, the regenerative braking power is limited in absolute value to about 5% of the maximum braking power (0.1 MW), in order to make the supercapacitors recover as much energy as possible during the braking phase. In this way two reference profiles are obtained to carry out the sizing: P_REF_B for the battery pack and P_REF_SC for the supercapacitors, as shown in Figure 18.

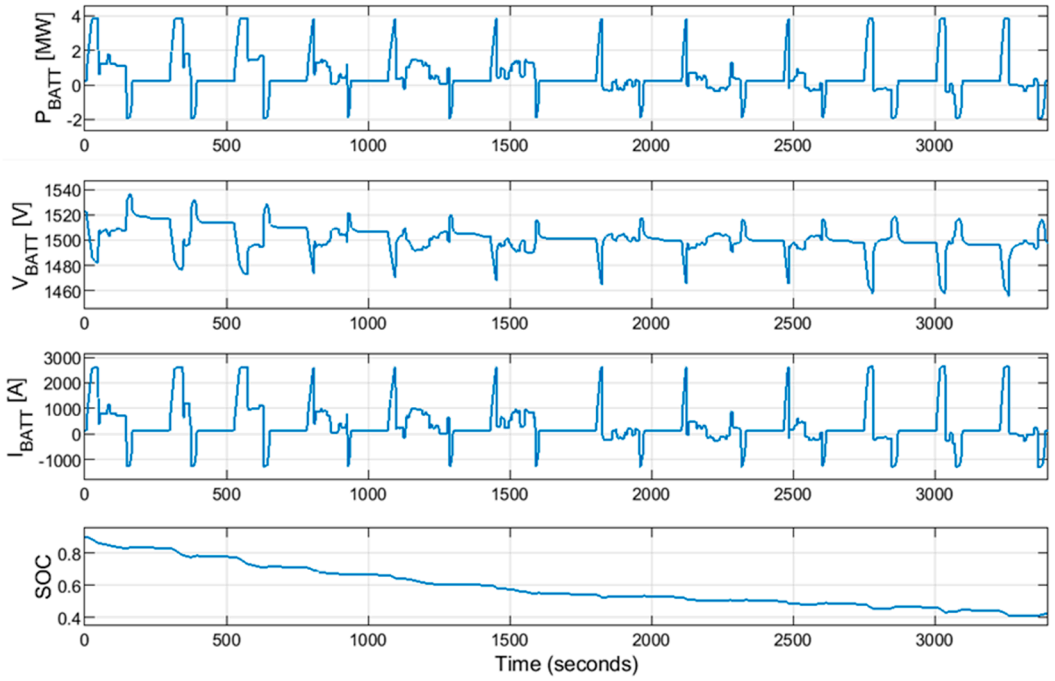

Figure 17. High autonomy ESS parameters-High-power lithium ion cells.

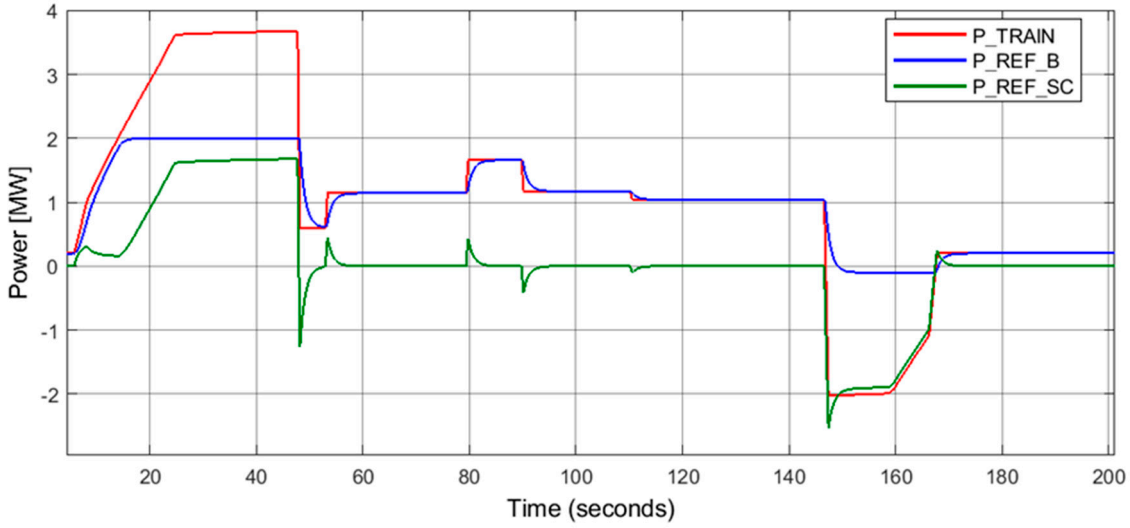

Figure 18. Power profiles H-ESS.

Carrying out the verification simulations of the H-ESS, it is observed in Figure 19a that the current required to the battery pack (in blue) tends to exceed the limits set by the manufacturer during discharge and is therefore limited to a lower current (in orange). Moreover, the supercapacitor SOC reaches too low values, as shown in Figure 19b. To avoid these situations, it is necessary to increase the quantity of parallel branches of high-energy lithium and supercapacitors cells, further increasing the total mass of the storage system. This hybrid solution is thus abandoned because it is too heavy.

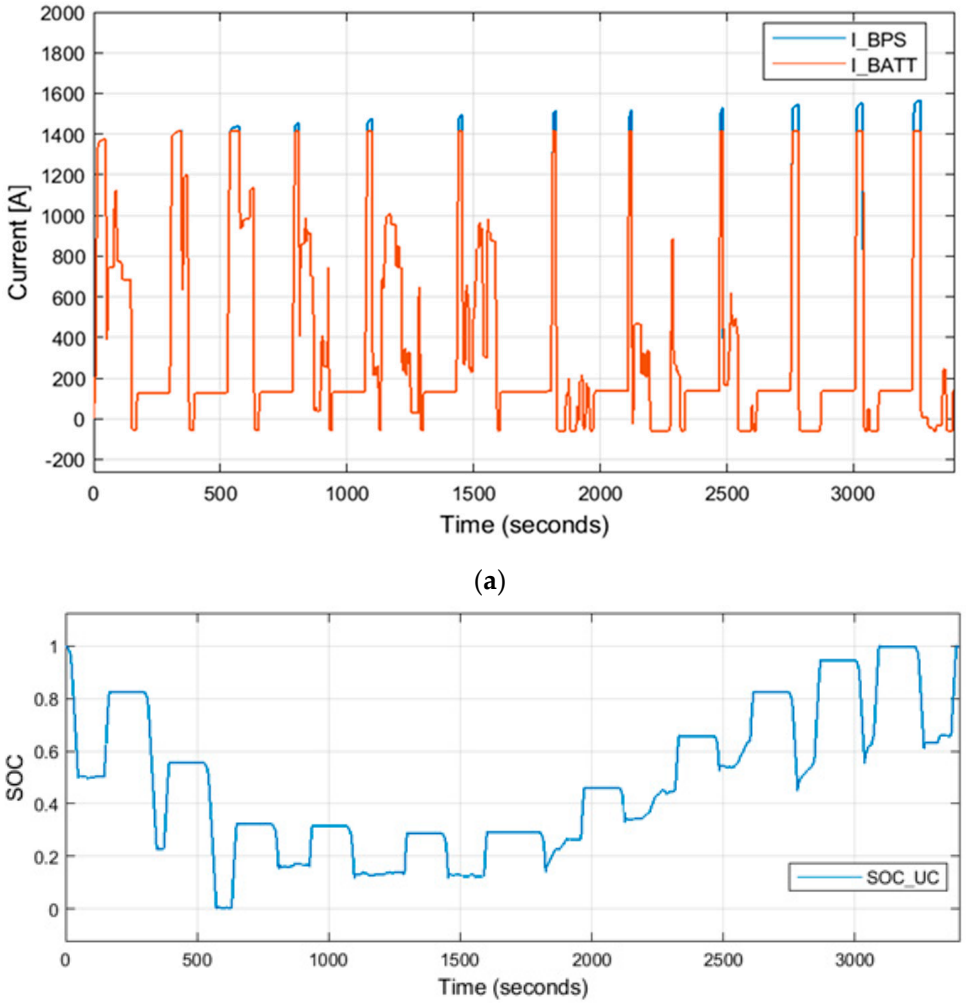

Figure 19. H-ESS: (**a**) Current required to the battery pack; (**b**) Supercapacitor pack SOC.

The ESS with recharge station implies an autonomy to go from Station A to Station B, where the recharge needs to be performed. According to this cycle, the energy to be supplied to the rolling stock is equal to 383 kWh. It has been considered the use of high-power lithium-ion cells and the sizing procedure results in a 640 kWh (425 Ah) battery pack, which does not exceed the limits set by the manufacturer. The recharge at Station B can be performed from the 30% to the 50% of the SOC, since it allows arriving to Station A within the available SOC range. Therefore, the recharge must have a duration of 6 min, at 2C rate, implying a recharge station of at least 1.4 MW.

In Figure 20 it is shown the charging time for both high autonomy ESS and ESS with recharge station, to be performed at Station A (in the electrified section). This recharge takes the SOC from 30% to 90% and it is performed, at 2C, in 18 min (LFP cells). Table 4 presents a synthesis of the viable on-board ESS scenarios, including the ESS impact in the energy required by the rolling stock because of the weight increase.

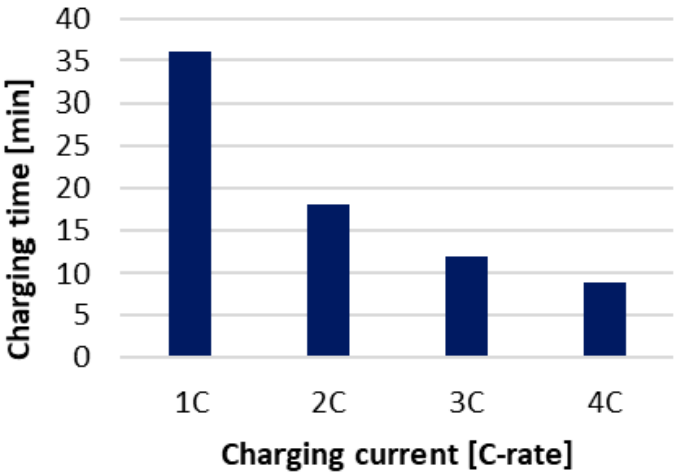

Figure 20. On-board ESS charging time.

Table 4. On-board ESS scenarios.

	High Autonomy ESS	ESS with Recharge Station
Rated capacity [Ah]	650	427.5
Rated capacity [kWh]	976	642
Available capacity [kWh]	586	385
ESS weight [t]	9	6
Train Performance energy impact [%]	3	2
Recharge power @2C (C-rate) [MW]	2.2	1.4

5.2.4. Economic Comparison

As reported in Section 2, the present value of total cost and the annual cost of energy are computed, considering the following hypothesis: an expected lifetime of 30 years; ESS lifetime of 10 years; an interest rate of 4% for electrification and 6% for ESS [45]; an average cost of electricity of 15 €/MWh [49]; charge efficiency equal to 90%; four daily connections between Station A–Station B. In Figure 21 it is shown the total cost (a) and the ACOE of the proposed scenarios. 3 kV DC electrification shows a present value of the total costs of approximately €13 M and an ACOE of over 700,000€ per year. Most of these costs come from the high investment cost necessary for the electrification, estimated at €10 M, as it is necessary to install a traction power substation, a contact line and carry out works such as track lowering in correspondence of tunnels already present in the route and raising of the overpasses. The ESS with recharge station has a present value of the total cost of approximately €7 M, considering the replacement of the storage system every 10 years (it will depend on the correct operation in charge/discharge phases), and the installation of the necessary system for charging. The ACOE of this solution is about 500,000€ per year, due to the lower costs associated with the charging station compared to those associated with the installation of TPS. Finally, the high autonomy ESS, with a total cost of €5.5 M and ACOE of 400,000€ per year, could be advantageous solution from the economic point of view, since it does not involve the installation of any infrastructure for the recharge.

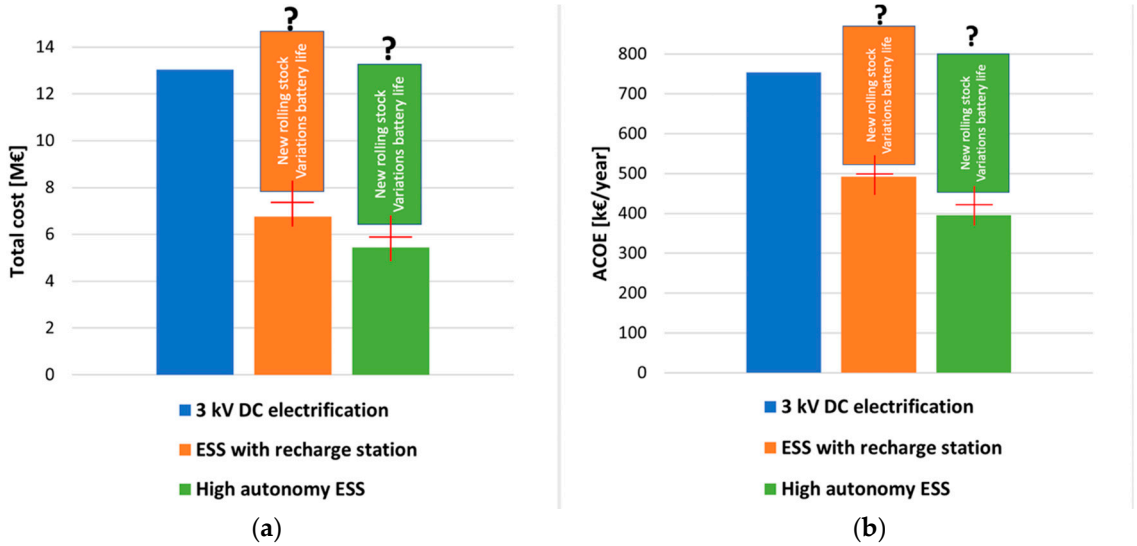

Figure 21. Different scenarios comparison: (**a**) Present value of total cost; (**b**) ACOE.

The main advantage of on-board ESS with high autonomy is that it does not require the installation of additional charging systems as this is provided for in the already electrified section of the railway line. Consequently, investment costs are limited. Moreover, on-board storage systems work with shallower charge and discharge cycles.

It should be emphasized, once again, that apparently the total costs linked to the solutions related to the use of trains with on-board storage would seem to be lower but it is necessary to underline that the total cost will strongly depend on the costs related to the construction of new rolling stock. Subsequently the real lifecycle of the batteries could lead to a further increase in costs due to their early replacement. However, investments in e-mobility lead to an increasing mass production of batteries. Consequently, if high demand growth is sustained, battery solutions are expected to be more profitable.

The feasibility of trains with on board ESS is similar to that of fully electrifying the ships that will sail the North Sea in the near future [63]. In both cases, current reliable solutions (i.e., electrified railway lines and heavy fuel oil powered shipping vessels, respectively) may lead to a previous hybridization stage before achieving the complete on-board energy supply system.

6. Conclusions

In the very near future more technical-economic comparisons between diesel/electrified railway and the use of trains with on-board energy storage systems will be carried out in order to define the best solution achievable from an environment and economic point of view in relation to different railways lines. It will be necessary define the adoption of these systems for expansion of already electrified railways, point-to-point connections, commuter transport systems and so on.

The times are becoming ripe and consequently the paper defines methodologies, procedures, simulation models considering the main economic aspects, in order to increase the scientific literature on these innovations that will be increasingly investigated.

The methodology and the model developed in this paper could help to define a series of aspect to consider when is necessary compare different system adoptable to modernize a railway line.

The paper shown numerical simulations on a real railway line that presents a 3 kV DC electrified section and a non-electrified section, currently covered by diesel-powered trains. Different types of ESS have been analyzed, evaluating the use of high-power lithium cells or high-specific lithium cells and supercapacitors. The models of the battery pack and supercapacitor pack have been implemented in the Matlab/Simulink environment. Three main scenarios have been evaluated for the non-electrified section: 3 kV DC electrification, on-board ESS with high autonomy and on-board ESS with recharge station.

The results showed that the use of trains equipped with on-board energy storage system could be a good solution, but from a preliminary economic point of view, today many cost parameter are still not well known. Consequently, over the years, through the first realizations and the monitoring of the operation, it will be possible to definite clarification of the costs, as well as they are well established and consolidated in the electrification at 3 kV DC.

It is also shown that the most suitable storage technology for the case under study is that of high-power lithium ion batteries. The on-board ESS with high autonomy presents an ACOE of about €400 k/year, apparently 40% less than the 3 kV DC electrification scenario (costs of new train manufacture, battery disposal are not taken into account). Since the case study concerns a single-track railway line in which maximum speeds are limited, two trains allow to cover the entire section without any impact on the service offered to passengers, given the charging times and autonomy of the chosen solution.

Finally, it should be noted that the electrification of railway lines represents a consolidated and highly reliable solution. Contrariwise, the use of trains equipped with on-board energy storage systems represents a solution currently being tested, which will take many years before a consolidation.

It will be very important to know the cost of the new trains equipped with ESS on board, taking into account the long homologation procedure until they are placed on the market, and the real behavior of the storage systems in relation to life expectancy.

Author Contributions: Conceptualization, R.L., A.R., G.G.B. and N.C.; methodology, R.L. and A.R.; software, R.L. and A.R.; validation, R.L. and A.R.; investigation, M.T.; data curation, M.T., A.R., G.G.B. and N.C.; writing—original draft preparation, M.T. and A.R.; writing—review and editing, M.T., A.R., G.G.B. and N.C.; visualization, R.L. and A.R. All authors have read and agreed to the published version of the manuscript.

Funding: This research received no external funding.

Conflicts of Interest: The authors declare no conflict of interest.

Abbreviations

$ACOE$	Annual cost of energy	E_B	Energy of battery
$ACOE_{ELE}$	Annual cost of energy of electrification	E_d^{TPS}	Energy supplied by the traction power substation in a day
$ACOE_{ESS}$	Annual cost of energy of energy storage system	$H\text{-}ESS$	Hybrid energy storage system
$C_{AH_{CELL_B}}$	Nominal capacity of the cell		Number of cells to be connected in the series
C_I^{ELE}	Capital cost of electrification	N_{PAR_B}	Number of branches to be connected in parallel
C_I^{ESS}	Capital cost of on-board ESS	$N_{SE_{SC}}$	Number of cells to be connected in series for supercapacitors
C_n^{ELE}	Annual operation costs of electrification	$N_{PAR_{SC}}$	Number of branches to be connected in parallel for supercapacitors
C_n^{ESS}	Annual operation costs of on-board ESS	OCV	Open circuit voltage
$C_{O\&M}^{ELE}$	Operation and maintenance (O&M) costs of electrification	O&M	Operation and maintenance
$C_{O\&M}^{ESS}$	Operation and maintenance (O&M) costs of on-board ESS	$P_{CELL_B}^{max}$	Maximum power that the single electrochemical cell can deliver
C_R^{ESS}	Replacement cost of the on-board ESS	$P_{CELL_{B_{CH}}}$	Maximum power that the single cell can absorb in the charging phase
CRF	Capital recovery factor	$P_{CELL_{B_{DIS}}}$	Maximum power that the single cell can give in the discharging phase
C_n^{TPS}	Annual costs associated with the maintenance of the traction power substation	R_{DIS}	The discharge C-rate
C_n^{CAT}	Annual costs associated with the maintenance of the catenary	SC	Supercapacitor
C_e	The average cost of electricity	SOC	State of charge
ESS	Energy storage system	TPS	Traction power substation
E_{SC}	Energy of supercapacitor	$U_{CELL_{SC}}$	Supercapacitor rated voltage

References

1. International Energy Agency. Rail. Available online: https://www.iea.org/reports/rail (accessed on 10 September 2020).
2. Electric vehicles from life cycle and circular economy perspectives. In *TERM 2018: Transport and Environment Reporting Mechanism (TERM) Report*; European Environment Agency: Luxembourg, 2018; Available online: https://www.eea.europa.eu/publications/electric-vehicles-from-life-cycle (accessed on 10 September 2020).
3. The First and Last Mile—The Key to Sustainable Urban Transport. In *Transport and Environment Report 2019*; EEA—European Environment Agency: Luxembourg, 2019; Available online: https://www.eea.europa.eu/publications/the-first-and-last-mile. (accessed on 10 September 2020).
4. Messagie, M.; Boureima, F.-S.; Coosemans, T.; Macharis, C.; Mierlo, J.V. A Range-Based Vehicle Life Cycle Assessment Incorporating Variability in the Environmental Assessment of Different Vehicle Technologies and Fuels. *Energies* **2014**, *7*, 1467–1482. [CrossRef]
5. UIC—International Union of Railways, «Railway Statistics Synopsis». Available online: https://uic.org/IMG/pdf/uic-statistics-synopsis-2019.pdf (accessed on 8 September 2020).
6. Kawamoto, R.; Mochizuki, H.; Moriguchi, Y.; Nakano, T.; Motohashi, M.; Sakai, Y.; Inaba, A. Estimation of CO_2 Emissions of Internal Combustion Engine Vehicle and Battery Electric Vehicle Using LCA. *Sustainability* **2019**, *11*, 2690. [CrossRef]
7. Hill, N. Impact Analysis of Mass EV Adoption and Low Carbon Adoption Intensity Fuels Scenarios. In Proceedings of the 13th Concawe Symposium, Antwerp, Belgium, 18–19 March 2019.
8. Kamargianni, M.; Li, W.; Matyas, M.; Schafer, A. A Critical Review of New Mobility Services for Urban Transport. *Transp. Res. Procedia* **2016**, *14*, 3294–3303. [CrossRef]
9. Cimen, S.G.; Gnilka, M.; Schmuelling, B. Economical, social and political aspects of e-mobility in Germany. In Proceedings of the 2014 Ninth International Conference on Ecological Vehicles and Renewable Energies (EVER), Monte, Torino, Italy, 15–16 June 2014; pp. 1–5. [CrossRef]
10. Franzò, S.; Chiaroni, D.; Chiesa, V.; Frattini, F. Emerging business models fostering the diffusion of E-mobility: Empirical evidence from Italy. In Proceedings of the 2017 International Conference of Electrical and Electronic Technologies for Automotive, Torino, Italy, 15–16 June 2017; pp. 1–5. [CrossRef]
11. Siemens. A New Era of Sustainable Road Freight Transport. 2020. Available online: https://new.siemens.com/global/en/products/energy/medium-voltage/solutions/emobility/emobility-latest-technologies.html (accessed on 20 September 2020).
12. Felez, J.; García-Sanchez, C.; Lozano, J.A. Control Design for an Articulated Truck with Autonomous Driving in an Electrified Highway. *IEEE Access* **2018**, *6*, 60171–60186. [CrossRef]
13. Xiao, S.; Zhang, C.; Luo, Y.; Wu, J.; Rao, Y.; Sykulski, J.K. A Study on the Detachment Characteristics of the Tramwave Catenary-Free Electrification System for Urban Traffic. *IEEE Trans. Plasma Sci.* **2020**, *48*, 3670–3678. [CrossRef]
14. Bombardier Transportation. Solutions and Technologies. 2020. Available online: https://www.bombardier.com/en/transportation/products-services.html (accessed on 20 September 2020).
15. Mayer, L. *Impianti Ferroviari*; CIFI: Rome, Italy, 2016; Volume 2.
16. Miyatake, M.; Haga, H.; Suzuki, S. Optimal speed control of a train with On-board energy storage for minimum energy consumption in catenary free operation. In Proceedings of the 2009 13th European Conference on Power Electronics and Applications, Barcelona, Spain, 8–10 September 2009; pp. 1–9.
17. Al-Ezee, H.; Sarath, T.; Taylor, I.; Daniel, S.; Schweickart, J. An On-board Energy Storage System for Catenary Free Operation of a Tram. *Renew. Energy Power Qual. J.* **2017**, *1*, 540–544. [CrossRef]
18. Steiner, M.; Klohr, M.; Pagiela, S. Energy storage system with ultracaps on board of railway vehicles. In Proceedings of the2007 European Conference on Power Electronics and Applications, Aalborg, Denmark, 2–5 September 2007; pp. 1–10. [CrossRef]
19. Ghaviha, N.; Campillo, J.; Bohlin, M.; Dahlquist, E. Review of Application of Energy Storage Devices in Railway Transportation. *Energy Procedia* **2017**, *105*, 4561–4568. [CrossRef]
20. Ogura, K. Test Results of a High Capacity Wayside Energy Storage System Using Ni-MH Batteries for DC Electric Railway at New York City Transit. In Proceedings of the 2011 IEEE Green Technologies Conference (IEEE-Green), Baton Rouge, LA, USA, 14–15 April 2011; pp. 1–6. [CrossRef]
21. Available online: https://www.globalmasstransit.net/archive.php?id=15973 (accessed on 8 September 2020).

22. Liu, X.; Li, K. Energy storage devices in electrified railway systems: A review. *Transp. Saf. Environ.* **2020**, *2*, 183–201. [CrossRef]
23. Hayashiya, H.; Masuda, M.; Noda, Y.; Suzuki, K.; Suzuki, T. Reliability analysis of DC traction power supply system for electric railway. In Proceedings of the 2017 19th European Conference on Power Electronics and Applications (EPE'17 ECCE Europe), Warsaw, Poland, 11–14 September 2017; pp. P.1–P.6. [CrossRef]
24. White, R.D. AC 25kV 50 Hz electrification supply design. In Proceedings of the 6th IET Professional Development Course on Railway Electrification Infrastructure and Systems (REIS 2013), London, UK, 3–6 June 2013; pp. 108–150. [CrossRef]
25. Fei, Z.; Konefal, T.; Armstrong, R. AC railway electrification systems—An EMC perspective. *IEEE Electromagn. Compat. Mag.* **2019**, *8*, 62–69. [CrossRef]
26. Jafri, N.H.; Gupta, S. An overview of Fuel Cells application in transportation. In Proceedings of the 2016 IEEE Transportation Electrification Conference and Expo, Asia-Pacific (ITEC Asia-Pacific), Busan, Korea, 1–4 June 2016; pp. 129–133. [CrossRef]
27. Rizzo, R.; Spina, I.; Boscaino, V.; Miceli, R.; Capponi, G. A Novel Fuel Cell-Based Power System Modeling Approach. In Proceedings of the 2013 European Modelling Symposium, Manchester, UK, 20–22 November 2013; pp. 370–374. [CrossRef]
28. Graber, G.; Galdi, V.; Calderaro, V.; Piccolo, A. Sizing and energy management of on-board hybrid energy storage systems in urban rail transit. In Proceedings of the 2016 International Conference on Electrical Systems for Aircraft, Railway, Ship Propulsion and Road Vehicles & International Transportation Electrification Conference (ESARS-ITEC), Toulouse, France, 2–4 November 2016; pp. 1–6. [CrossRef]
29. Iwase, T.; Kawamura, J.; Tokai, K.; Kageyama, M. Development of battery system for railway vehicle. In Proceedings of the 2015 International Conference on Electrical Systems for Aircraft, Railway, Ship Propulsion and Road Vehicles (ESARS), Aachen, Germany, 3–5 March 2015; pp. 1–6. [CrossRef]
30. Unique Energy Hub. Universal Ragone Plot. Available online: https://uenergyhub.com/info/universal-ragone-plot/ (accessed on 6 September 2020).
31. Sadoun, R.; Rizoug, N.; Bartholomeüs, P.; Barbedette, B.; Le Moigne, P. Optimal sizing of hybrid supply for electric vehicle using Li-ion battery and supercapacitor. In Proceedings of the 2011 IEEE Vehicle Power and Propulsion Conference, Chicago, IL, USA, 6–9 September 2011; pp. 1–8. [CrossRef]
32. Mesbahi, T.; Rizoug, N.; Bartholomeüs, P.; Sadoun, R.; Khenfri, F.; Le Moigne, P. Optimal Energy Management for a Li-Ion Battery/Supercapacitor Hybrid Energy Storage System Based on a Particle Swarm Optimization Incorporating Nelder–Mead Simplex Approach. *IEEE Trans. Intell. Veh.* **2017**, *2*, 99–110. [CrossRef]
33. Ostadi, A.; Kazerani, M.; Chen, S. Optimal sizing of the Energy Storage System (ESS) in a Battery-Electric Vehicle. In Proceedings of the 2013 IEEE Transportation Electrification Conference and Expo (ITEC), Detroit, MI, USA, 16–19 June 2013; pp. 1–6. [CrossRef]
34. Sadoun, R.; Rizoug, N.; Bartholomeüs, P.; Le Moigne, P. Optimal architecture of the hybrid source (battery/supercapacitor) supplying an electric vehicle according to the required autonomy. In Proceedings of the 2013 15th European Conference on Power Electronics and Applications (EPE), Lille, France, 2–6 September 2013; pp. 1–7. [CrossRef]
35. Cao, J.; Emadi, A. A new battery/ultra-capacitor hybrid energy storage system for electric, hybrid and plug-in hybrid electric vehicles. In Proceedings of the 2009 IEEE Vehicle Power and Propulsion Conference, Dearborn, MI, USA, 7–11 September 2009; pp. 941–946. [CrossRef]
36. Ostadi, A.; Kazerani, M. A Comparative Analysis of Optimal Sizing of Battery-Only, Ultracapacitor-Only, and Battery–Ultracapacitor Hybrid Energy Storage Systems for a City Bus. *IEEE Trans. Veh. Technol.* **2015**, *64*, 4449–4460. [CrossRef]
37. Tummakuri, V.; Chelliah, T.R.; Ramesh, U.S. Sizing of Energy Storage System for A Battery Operated Short Endurance Marine Vessel. In Proceedings of the 2020 IEEE International Conference on Power Electronics, Smart Grid and Renewable Energy (PESGRE2020), Cochin, India, 2–4 January 2020; pp. 1–6. [CrossRef]
38. Balsamo, F.; Lauria, D.; Capasso, C.; Veneri, O.; Pede, G. Main issues with the design of batteries to power full electric water busses. In Proceedings of the 2016 AEIT International Annual Conference (AEIT), Capri, Italy, 5–7 October 2016; pp. 1–6. [CrossRef]
39. Bolonne, S.R.A.; Chandima, D.P. Sizing an Energy System for Hybrid Li-Ion Battery-Supercapacitor RTG Cranes Based on State Machine Energy Controller. *IEEE Access* **2019**, *7*, 71209–71220. [CrossRef]

40. Brenna, M.; Foiadelli, F.; Stocco, J. Battery Based Last–Mile Module for Freight Electric Locomotives. In Proceedings of the 2019 IEEE Vehicle Power and Propulsion Conference (VPPC), Hanoi, Vietnam, 14–17 October 2019; pp. 1–6. [CrossRef]
41. Weiss, H.; Winkler, T.; Ziegerhofer, H. Large lithium-ion battery-powered electric vehicles—From idea to reality. In Proceedings of the 2018 ELEKTRO, Mikulov, Czech Republic, 21–23 May 2018; pp. 1–5. [CrossRef]
42. Royston, S.J.; Gladwin, D.T.; Stone, D.A.; Ollerenshaw, R.; Clark, P. Development and Validation of a Battery Model for Battery Electric Multiple Unit Trains. In Proceedings of the IECON 2019—45th Annual Conference of the IEEE Industrial Electronics Society, Lisbon, Portugal, 14–17 October 2019; pp. 4563–4568. [CrossRef]
43. Construcciones y Auxiliar de Ferrocarriles (CAF) S.A. Greentech, CAF's Solution to the Catenary-Free Tram. Available online: https://www.caf.net/en/ecocaf/nuevas-soluciones/tranvia-greentech.php (accessed on 6 September 2020).
44. Bombardier Transportation. World Premiere: Bombardier Transportation Presents a New Battery-Operated Train and Sets Standards for Sustainable Mobility. 2018. Available online: https://rail.bombardier.com/en/newsroom/press-releases.html/bombardier/news/2018/bt-20180912-world-premiere–bombardier-transportation-presents-a/en (accessed on 6 September 2020).
45. Bombardier Transportation. E-Mobility and Battery Technology. 2020. Available online: https://rail.bombardier.com/en/solutions-and-technologies/urban/e-mobility-battery-technology.html (accessed on 6 September 2020).
46. Graber, G.; Calderaro, V.; Galdi, V.; Piccolo, A.; Lamedica, R.; Ruvio, A. Techno-economic Sizing of Auxiliary-Battery-Based Substations in DC Railway Systems. *IEEE Trans. Transp. Electrif.* **2018**, *4*, 616–625. [CrossRef]
47. Lamedica, R.; Ruvio, A.; Galdi, V.; Graber, G.; Sforza, P.; GuidiBuffarin, G.; Spalvieri, C. Application of battery auxiliary substations in 3kV railway systems. In Proceedings of the 2015 AEIT International Annual Conference (AEIT), Naples, Italy, 14–16 October 2015; pp. 1–6. [CrossRef]
48. Ruiz-Cortés, M.; Romero-Cadaval, E.; Roncero-Clemente, C.; Barrero-González, F.; González-Romera, E. Energy management strategy to coordinate batteries and ultracapacitors of a hybrid energy storage system in a residential prosumer installation. In Proceedings of the 2017 International Young Engineers Forum (YEF-ECE), Almada, Portugal, 5 May 2017; pp. 30–35. [CrossRef]
49. Lee, J.; Ahn, J.; Lee, B.K. A novel li-ion battery pack modeling considering single cell information and capacity variation. In Proceedings of the 2017 IEEE Energy Conversion Congress and Exposition (ECCE), Cincinnati, OH, USA, 1–5 October 2017; pp. 5242–5247. [CrossRef]
50. Gattuso, D.; Restuccia, A. A Tool for Railway Transport Cost Evaluation. *Procedia Soc. Behav. Sci.* **2014**, *111*, 549–558. [CrossRef]
51. Baumgartner, J.P. Prices and Costs in the Railway Sector. Laboratoire d'Intermodalité des Transports Et de Planification 2001, Lausanne. Available online: http://archiveweb.epfl.ch/litep.epfl.ch/files/content/sites/litep/files/shared/Liens/Downloads/Divers/Baumgartner_Couts_chf_2001_e.pdf (accessed on 6 September 2020).
52. Ceraolo, M.; Giglioli, R.; Lutzemberger, G. Prove Sperimentali e Ciclo Semplificato di un Sistema di Accumulo Per Una Tramvia. ENEA—National Agency for New Technologies. 2015. Available online: https://www.enea.it/it/Ricerca_sviluppo/documenti/ricerca-di-sistema-elettrico/accumulo/2014/rds-par2014-175.pdf (accessed on 6 September 2020).
53. Marignetti, F. *La Trazione Ferroviaria: I Sistemi a Guida Vincolata*; Società Editrice Esculapio: Bologna, Italy, 2018.
54. Ehsani, M.; Yimin, G.; Emadi, A. *Modern Electric, Hybrid Electric and Fuel Cell Vehicles Fundamentals, Theory and Design Second Edition*; CRC Press: Boca Raton, FL, USA, 2010.
55. Chu, H.; Wang, X.; Mu, X.; Gao, M.; Liu, H. Research on Optimal Configuration of Hybrid Energy Storage Capacity Based on Improved Particle Swarm Optimization Algorithm. In Proceedings of the 2019 IEEE 4th Advanced Information Technology, Electronic and Automation Control Conference (IAEAC), Chengdu, China, 20–22 December 2019; pp. 2030–2036. [CrossRef]
56. LeBel, F.; Trovao, J.P.; Boulon, L.; Sari, A.; Pelissier, S.; Venet, P. Lithium–Ion Cell Empirical Efficiency Maps. In Proceedings of the 2018 IEEE Vehicle Power and Propulsion Conference (VPPC), Chicago, IL, USA, 27–30 August 2018; pp. 1–4. [CrossRef]
57. Calderaro, V.; Galdi, V.; Graber, G.; Lamberti, F.; Piccolo, A. A sizing method for economic assessment of II-life batteries for power system applications. In Proceedings of the 2017 IEEE Power & Energy Society General Meeting, Chicago, IL, USA, 16–20 July2017; pp. 1–5. [CrossRef]

58. D'Orazio, A.; Elia, S.; Santini, E.; Tobia, M. Succor System and Failure Indication for the Starter Batteries of Emergency Gensets. *Period. Polytech. Electr. Eng. Comput. Sci.* **2020**, *64*, 412–421. [CrossRef]
59. Boccaletti, C.; Elia, S.; Salas, M.E.F.; Pasquali, M. High reliability storage systems for genset cranking. *J. Energy Storage* **2020**, *29*, 101336. [CrossRef]
60. Capasso, A.; Lamedica, R.; Ruvio, A.; Giannini, G. Eco-friendly urban transport systems. Comparison between energy demands of the trolleybus and tram systems. *Ing. Ferrov.* **2014**, *69*, 329–347.
61. Capasso, A.; Ceraolo, M.; Lamedica, R.; Lutzemberger, G.; Ruvio, A. Modelling and simulation of tramway transportation systems. *J. Adv. Transp.* **2019**, *2019*, 4076865. [CrossRef]
62. Lamedica, R.; Gatta, F.M.; Geri, A.; Sangiovanni, S.; Ruvio, A. A software validation for dc electrified transportation system: A tram line of Rome. In Proceedings of the 2018 IEEE International Conference on Environment and Electrical Engineering and 2018 IEEE Industrial and Commercial Power Systems Europe (EEEIC/I&CPS Europe), Palermo, Italy, 12–15 June 2018; pp. 1–6. [CrossRef]
63. Savard, C.; Nikulina, A.; Mécemmène, C.; Mokhova, E. The Electrification of Ships Using the Northern Sea Route: An Approach. *J. Open Innov. Technol. Mark. Complex.* **2020**, *6*, 13. [CrossRef]